Magnetism and Superconductivity in Hydrogenated Graphite Foils

Nadina Gheorghiu, Charles R. Ebbing, and Timothy J. Haugan

***Abstract*—We have previously found magnetism and superconductivity in hydrogenated graphite [Gheorghiu, et al. (2020)]. Herein, the two phenomena are observed in hydrogenated graphite foils. As the strength of the magnetic field is increased, the temperature-dependent magnetization shows several transitions between different states: from Néel paramagnetic, to antiferromagnetic, to ferromagnetic superconductor, to high-temperature superconductor with the critical temperature for the dominant phase $T_c \sim$ 50–60 K. The latter might be an orbital paramagnetic glass ordering of π Josephson-coupled SC domains akin to a macroscopic quantization of the system. The magnetization loops show the kink feature characteristic to granular SC. The ferromagnetism is observed up to room temperature. Thus, we observe both magnetism and superconductivity in hydrogenated graphite foils.**

***Index Terms*—High-temperature superconductors, ferromagnetic materials, antiferromagnetic materials, paramagnetic materials, organic compounds, graphite, hydrogen.**

I. Introduction

MAGNETISM and superconductivity (SC) were thought as mutually exclusive physical phenomena. In cuprates, high-temperature superconductivity (HTSC) emerges from tuning the charge-doping of the parent phase, an antiferromagnetic (AFM) Mott insulator. The emergence of new SC materials like the (iron-based) pnictides showed the important role played by long-range magnetic spin correlations. A ferromagnetic (FM) domain can transfer the magnetically stable spin-triplets into the neighboring nonmagnetic domains and the latter becomes SC. Long-range proximity effects are established at the SC/FM interfaces. Anisotropic materials might contain magnetically soft/hard or FM/AFM domains that are interfacially coupled, leading to the formation of quasi-Bloch walls [2]. FM and SC can actually coexist in graphite and other carbon (C)- based materials [3], [4], [5], [6], [7], [8]. Can these low-weight materials reach higher T_c, maybe even higher than the 200 K found in a specially prepared phase of the rare-earth material YBCO [9]?

In the BCS theory [10], the attractive interactions between electrons are explained as mediated by the lattice excitations (phonons). For HTSC materials, it is the *e*-*e* correlations rather than *e*-phonon interactions that lead to high T_c. In [1], we have proposed that HTSC in hydrogenated graphitic fibers could be explained by the Little model for HTSC in organic materials [11]. The Little model considers a molecular arrangement consisting of two parts: a) a long chain called the spine, in which the electrons fill various states and may or may not form a conducting system; b) a series of arms or side chains attached to the spine. The treatment with octane results in the free protonation of octane at graphite's interfaces [12], [13]. The resulted superacidic protons (H^+) move freely (with no activation energy) on the graphite surfaces, giving rise to HTSC. Thus, when the Little model is applied to the H-C foil, one can imagine that the spines are in the C planes with the protons as the arms or side chains. The free protons are shared by all C atoms in the plane to which the arms are connected thus the protons mediate the *e*-*e* correlations. We have found that the magnetic field leads to SC correlations in hydrogenated graphite and other C-based materials [1], [14], [15], [16].

In this research, we are finding magnetic and SC transitions in hydrogenated graphite foils. These results reinforce our previous research on FM and SC properties of hydrogenated graphitic fibers [1], [17], where the quantum phenomenon known as 2D weak localization can turn some of the *e*-*e* interactions into SC correlations [18]. While the σ electrons are localized, the π electrons are free to move like conduction electrons in metals and their long-range correlations result in FM. In graphite, there are intrinsic AFM correlations between unlike sublattices (ABAB …) and FM correlations between like sublattices (AAA … or BBB …) [19]. Hydrogenated graphene was predicted to be FM [20]. We have previously found both magnetism and SC in oxygen-implanted C−based materials [14], [15] as well as in boron-doped C−based materials [16], with $T_c \sim$ 50−80 K for the dominant SC fraction. Interestingly, the shielding fraction, hence T_c, increases with the number of benzene rings [21]. The results presented here are in agreement with our previous work, thus confirming that hydrogenated graphite is a FM HTSC.

II. Experiment

Graphite foil (Graphtek) square samples with dimensions 2 mm × 2 mm × 1 mm have undergone hydrogenation via doping by a hydrocarbon (octane, C_8H_{18}). The graphite foil

Received 24 September 2024; revised 16 December 2024; accepted 14 January 2025. Date of publication 24 January 2025; date of current version 14 February 2025. This work was supported in part by The Air Force Office of Scientific Research (AFOSR) under Grant LRIR #14RQ08COR and Grant LRIR #18RQCOR100 and in part by Air Force Research Laboratory within the Aerospace Systems Directorate (AFRL/RQ). *(Corresponding author: Nadina Gheorghiu.)*

Nadina Gheorghiu is with Universal Energy Systems (UES, Inc.), Dayton, OH 45432 USA (e-mail: nadina.gheorghiu@yahoo.com).

Charles R. Ebbing is with Universal Energy Systems (UES, Inc.), Dayton, OH 45432 USA, and also with the University of Dayton Research Institute, Dayton, OH 45469-0073 USA (e-mail: charles.ebbing@udri.edu).

Timothy J. Haugan is with Air Force Research Laboratory, Dayton, OH 45433 USA (e-mail: timothy.haugan@us.af.mil).

Color versions of one or more figures in this article are available at https://doi.org/10.1109/TASC.2025.3533460.

Digital Object Identifier 10.1109/TASC.2025.3533460

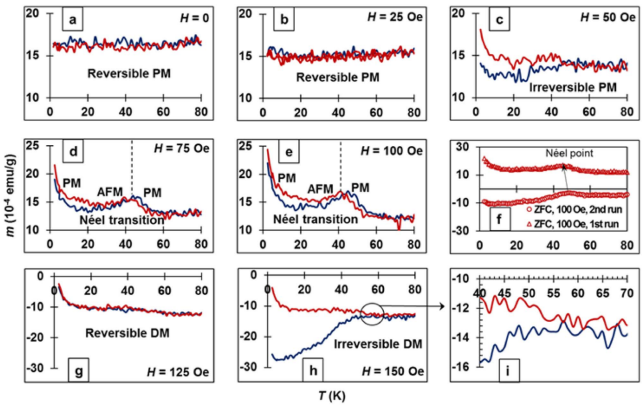

Fig. 1. ZFC (in blue) and FC (in red) low-field data for the H-C foil.

was soaked in octane for seven months and at room temperature. The resulted sample is referred as H-C foil. Here, the mass was 7.8 mg for the C foil and 7.7 mg for the H-C foil, respectively. The mass difference can be explained as follows: The H-C foil is chemically different than the C foil, as the octane is molecularly broken at the graphite surface. This results in the formation of molecular hydrogen, methane, and ethane, hence the protonation of the basal graphite surface by octane. In addition, even a gentle handling of the sample leads to a small loss of mass. Using the vibrating sample magnetometry option of the Physical Properties Measurement System (PPMS) model 6500 (Quantum Design), magnetization measurements were carried out in the 1.9 K–300 K temperature (T) range and for magnetic fields of induction B up to 9 T applied perpendicularly to the graphite layers. The PPMS sensitivity was at least 0.5×10^{-6} emu, while samples' magnetization was 50–100% larger. While usually, though not always, both transport and magnetization experiments are done in order to probe SC signatures in SC samples, here we have chosen to consider only results from magnetization experiments. The superconducting interpretation of the observed magnetic-field hysteresis is supported by the observation of thermomagnetic hysteresis that can differentiate a ferromagnetic from a superconducting behavior. The results from transport measurements can be found in an earlier publication [22].

III. Results and Discussion

A. Temperature-Dependent Magnetization

The magnetization $m(T)$ data is shown in Fig. 1. Upon incrementally increasing the strength of the magnetic field H from 0 to 150 Oe, several important magnetic transitions occur in the H-C foil: from reversible to irreversible PM (Fig. 1(a)–(c)), to slightly irreversible PM-AFM Néel transition (Fig. 1(d)–(f)), to reversible diamagnetism (DM) (Fig. 1(g)), and to irreversible DM (Fig. 1(h)–(i)). The Néel transition temperature is $T_N \simeq 44$ K (Fig. 1(d)–(f)). Significantly, in high H, the Meissner fraction becomes dominant and the H-C foil becomes SC below $T_c \simeq 57$ K (Fig. 1(h)–(i)). The initially trapped magnetic flux is expelled. In addition, we observe a low-T upturn of the zero-field cooled (ZFC) and the field-cooled (FC) curves. This reentrant PM was observed in other high-T_c systems [23]. The Meissner fraction depends strongly on the strength of the applied field. In the high-field limit, the trapped flux fraction can be comparable to and eventually can cancel out the DM shielding fraction. This kind of Meissner effect, PM by nature, is due to the trapping of magnetic flux [24]. On decreasing T, the magnetic flux captured at the third (surface) critical field inside the SC sheath compresses into a smaller volume, thus allowing extra flux to penetrate at the surface [25]. The PM Meissner effect is a general property of a small SC, being enhanced in a plate geometry such as our graphite foil here. From all the evidence, HTSC occurs in the H-C materials at the interfaces, i.e., weak SC links are formed across the grain boundaries and/or across defect surfaces within the grains. Flux trapping and not pinning is the main mechanism for hysteresis in granular HTSC. At the SC/FM interfaces, the spin-orbit coupling induces spontaneous vortices (in $H = 0$) that are pinned along the edges of the FM and is reinforcing the SC state [26]. Moreover, in granular SC (type II SC), the occurrence of the PM Meissner effect proves the existence of π Josephson-coupled SC domains. The PM Meissner effect, known also as the Wohlleben effect [27], [28], was found to be inherent to granular SC [29]. In small topological (unconventional) SC, granular SC in particular, the intrinsic inhomogeneity can result in PM because of the odd-frequency Cooper pairs at the surface of the small SCs that are accompanied by zero-energy surface Andreev bound states [30]. Indeed, as we have found in [1] for hydrogenated graphitic fibers, the excitonic gap at $T_c = 50$ K suggested interference of chiral asymmetric Andreev edge states and crossed Andreev conversion. The reentrant PM can be clearly seen to dominate over DM below a temperature $T_p \leq 20$ K. Also, when Andreev bound states appear at the interface, the direction of the induced magnetization is opposite to that without Andreev bound states [31]. A singlet-triplet spin conversion results in sign change for the magnetization. The spin structure of the dominant Cooper pair determines the direction of the induced magnetization. Notice also that in magic-angle twisted bilayer and trilayer graphene there is a superposition of singlet (s-wave) and spin-triplet (p-wave) pairing [32]. The reentrant SC is observed in the trilayer case as well as in the hydrogenated graphite here. Moreover, spontaneous misfit of graphite's interfaces leads to a nearly flat energy band. The topological origin of the flat band, which can host both FM and HTSC states, can be understood in terms of the pseudo-magnetic field created by strain [33]. Deintercalated KC_8 showed T_c anomalies even above room-T and FM above 400 K [34]. Those findings as well as ours [1], [14] confirm that disordered C-allotropes with grain size 50–100 nm can show both FM and a relatively small fraction Meissner SC.

The PM is actually metastable. At a second run under the same H, $m < 0$, and a cusp left from the Néel point can still be seen, though at a higher value $T \simeq 49$ K (Fig. 1(f)). The cusp can be attributed to blocked superparamagnetism (SPM) and a FM order instead. The change in the sign of m from + to − shows that the trapped magnetic flux was removed from the system, which is now being driven into the SC state, as a more stable state than the PM one.

Upon further increasing H, m becomes again positive and the PM-AFM Néel transition reemerges at the same transition temperature $T_N \simeq 44$ K (Fig. 2). Several magnetic transitions

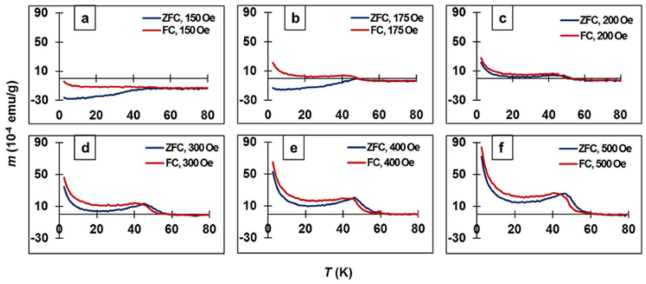

Fig. 2. ZFC (in blue) and FC (in red) high-field data for the H-C foil. For comparison with Fig. 1, the $H = 150$ Oe data was also included.

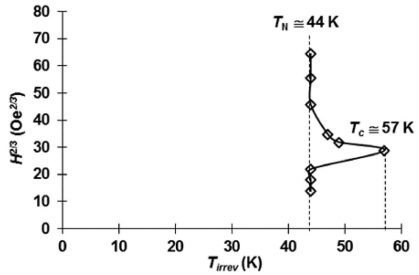

Fig. 3. The H-C foil is not a conventional glass system, as H2/3(T) is not an Almeida-Thouless line. The reentrance of PM followed by more PM-AFM Néel transitions suggests that the H-C foil might be an orbital PM glass HTSC, where orbital PM order and SC order coexist without the meissner effect.

are observed: irreversible DM (Fig. 2(a)), to irreversible PM-DM (Fig. 2(b)), to practically reversible PM (Fig. 2(c)), to slightly irreversible PM-AFM Néel transition (Fig. 2(d)–(f)). Fig. 2(b) shows the Wohlleben effect mentioned before. An increase in H has a direct effect on the intergranular currents, which contribution to m is either PM or DM. Thus, at high H, a reentrant PM order emerges alongside the SC order. As Fig. 3 shows, this spin-glass system's irreversible temperature $T_{\rm irrev}$ does not vary linearly with $H^{2/3}$ accordingly to the Almeida-Thouless scaling law. While the competition between the FM and AFM orders leads to magnetic frustrations and thus spin glass behavior, the nonlinear $H^{2/3}(T_{\rm irrev})$ suggests that we are possibly dealing with something different than a conventional long-range spin-glass behavior in a mean-field system. The behavior for $H \sim 150$ Oe (upper line above $T_c \simeq 57$ K) is similar to the $H - T_c$ line in [23] for a granular SC. The reentrance of PM and of the PM-AFM Néel transition can be explained by considering that the H-C foil is an orbital PM glass HTSC, where orbital PM and SC orders coexist without the Meissner effect [35]. After all, interlayer interaction in graphite can lead to enhanced PM orbital effect. The crystal-like orbital PM glass has chaotically distributed circular currents that can decrease and increase in time or even change direction (i.e., have orbital moment flips). The rate of change for these currents will depend on the local dissipation in the weak links that is due to impurities and the local H, which in turn will depend on the values of other orbital currents. The SC regions form thick rings of Josephson junctions and the magnetic flux going through the interior of the SC rings is a chaotic line (linear, circular, other), i.e., it is a topological object. Thus, the system is an orbital PM glass and a SC at the same time, moreover, it can be a HTSC. In addition, granular

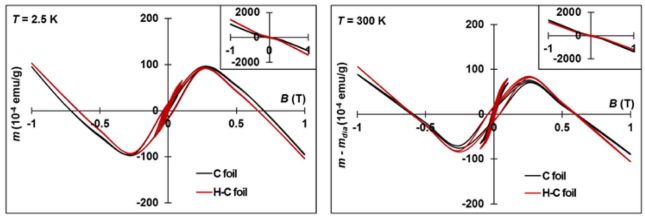

Fig. 4. High-field magnetization loops m(B) for T = 2.5 K and T = 300 K. Legend: raw C foil in black and H-C foil in red. DM background included (left) vs. DM background (inset) subtracted (right).

disordered HTSC might have the sign of some of their Josephson loops reversed when π-contacts are being created between SC grains via magnetic impurities. In the H-C foil here, itinerant FM is introduced in the system by octane with its freely moving H^+ (protons) on graphite's interfaces. Thus, the Josephson junction SC (JJSC) loops might have π-contacts. The formation of orbital PM glass is conditioned as follows: a) the JJSC rings with an even number of π-contacts give constant negative magnetic susceptibility, i.e., conventional Meissner response, while b) the JJSC rings with an odd number of π-contacts give (positive) PM susceptibility, which is proportional to $1/H$. Clearly, $\chi_{\rm m} \to 0$ as $H \to 0$ (abnormal response). At any number of JJSC rings, there will exist a small H for which the rings will give the main contribution to $\chi_{\rm m}$, which will be PM. The systems behavior is of a magnet with local orbital magnetic moment. On the other hand, the magnitude of the anti-Meissner signal decreases with increasing H and, for sufficiently large H, $\chi_{\rm m} < 0$, i.e., there is a DM Meissner effect. As Figs. 1-2 show, SC dominates over PM for 100 Oe $< H <$ 200 Oe. The rather small m observed for $H \sim$ 175–200 Oe (Fig. 2(c)) suggests a possible clustering of SPM order for field strengths smaller than needed for the reentrant PM that eventually will coexists with a SC order for $H \sim 300$ Oe. An intermediate SPM order can be seen as transitory form of magnetism proceeding the reentrance of orbital PM glass coexisting with SC. A persistent AFM/FM background for temperatures up to 50–60 K [1], which are coming from the free H^+ protons, might favor the occurrence of different magnetic orders, as well as the orbital glass behavior.

For moderate field strengths $H \geq 200$ Oe, the PM dominates. We observe both reentrant PM and more PM-AFM Néel transitions in the H-C foil, the latter occurring at the same $T_{\rm N} \simeq 44$ K (Fig. 2(d)–(f)). To our knowledge, these are completely new features, for which a new mechanism would be needed to explain both the coexistence of SC and orbital glass PM as well as the reentrant features observed in the H-C system. In high magnetic fields, the SC and the PM orbital glass are decoupled when the field direction is reversed and either DM ($\chi_{\rm m} < 0$) or PM ($\chi_{\rm m} > 0$) wins (Fig. 1). Important, T_c found here is close to the mean-field T_c for SC correlations in metallic-H multilayer graphene or highly oriented pyrolytic graphite, $T_c \sim 60$ K [36].

High-field magnetization loops $m(B)$ at temperatures $T =$ 2.5 K and $T = 300$ K are shown in Fig. 4. In order to separate the SC/FM response from the huge DM background, the sample DM response to a high field ($B = 1$ T, inset) was subtracted from the initial data (see inset). In high magnetic fields, the $m(B)$ loops are lines and show practically no hysteresis, reflecting the internal DM of the graphite samples. Thus, the linear $m(B)$

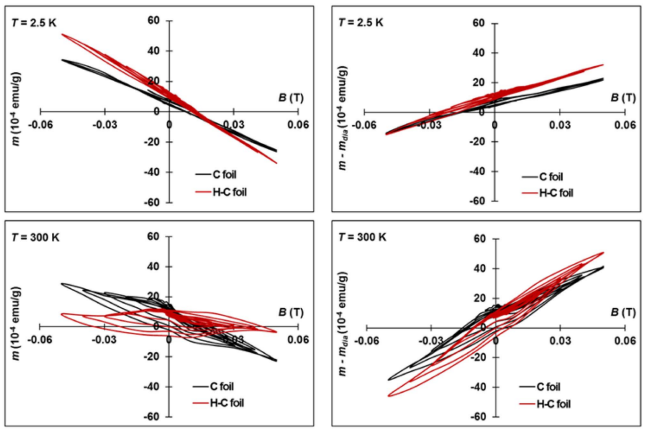

Fig. 5. Low-field magnetization loops m(B) for T = 2.5 K and T = 300 K. DM background included (left) vs. DM background (inset) subtracted (right). While both FM and SC are observed, the hysteresis decreases at low T. The asymmetry of these m(B) loops reflects the granular nature of the material.

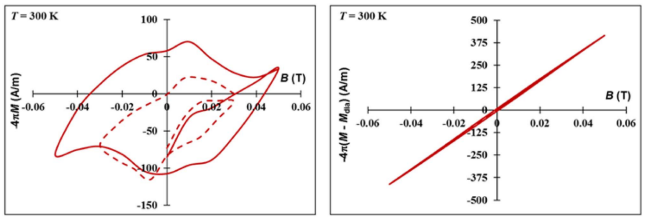

Fig. 6. Magnetic moment at T = 300 K with (left) and without (right) the DM background.

data for high values of B was subtracted from the $m(B)$ data for low values of B. Several important features we observe with these $m(B)$ loops: a) they have both FM and DM trends for $T < 300$ K, suggesting that the Curie temperature for these H-C foils is higher than the room temperature; b) after the subtraction of the DM background, they have an oscillatory dependence on the field, confirming the existence of the PM Meissner effect and surface SC, the latter showing metastability that is due to the coexistence of multi-quanta vortex states ($L\Phi_0$, $\Phi_0 = h/2e$, $L > 1$) and single quantum ($L = 1$, or Abrikosov) vortices [37]; c) as T goes up, the FM component increases at the expense of the PM component.

B. Magnetization Loops

Low-field $m(B)$ loops are shown in Fig. 5. There are several important features: a) At low T, the loops are not hysteretic, a characteristic of soft materials such as graphite foil; b) both the FM and the SC, or the FMSC, are pronounced in the H-C foil as compared to the C foil; c) the $m(B)$ loops show the "fishtail anomaly" (kink) feature characteristic to granular SC [38]; d) the hysteresis increases with the temperature and the FMSC becomes more evident beyond the low-T PM.

A couple of low-field $m(B)$ loops are shown in in Fig. 6. The known conversion factor was used: 1 emu $= 10^{-3}$ A·m^2. At $T =$ 300 K, the sample clearly is both DM and FM. The absence of points on the $m(B)$ loops that should correspond to B_{c1} and B_{c2} is due to the fact that the SC DM was subtracted, thus leaving out the FM behavior. Magnetic hysteresis comes mainly from

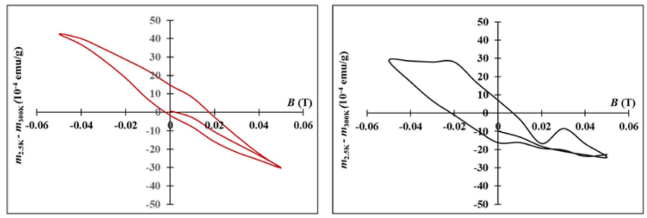

Fig. 7. Difference between the magnetic moment at $T = 2.5$ K and the one at $T = 300$ K for the H-C foil (left) and the C foil (right).

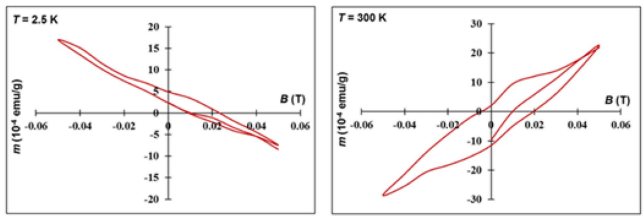

Fig. 8. Difference between the magnetic moment of the C foil and the magnetic moment for the H-C foil at $T = 2.5$ K (left) and at $T = 300$ K (right), respectively.

the DM component (including the SC component). For the inner loop, the critical values for the magnetic induction of this type II SC is of the order of few tens of mT, $B_{c1} \simeq 10$ mT and $B_{c2} \simeq 30$ mT. We use these values to estimate the penetration depth $\lambda \sim 250$ nm and the coherence length $\xi \sim 100$ nm. The ratio $\kappa = \lambda/\xi \simeq 2.5 > 0.42$ tells us that there is a SC surface layer for which a third maximum field B_{c3} can be defined [39] such that $B_{c3} = 2.4\kappa B_{c1} = 1.7B_{c2}$. Here, $B_{c3} \simeq 51$–60 mT. For ideal samples, the nucleation of SC regions is energetically favored to start from the samples' surface. In non-ideal samples like the ones here, the nucleation of SC regions in decreasing field is rather initiated from volume defects. It is possible that a bulk SC state (hugely-gaped) is found at $T_c \simeq 50$–60 K, while surface (topological) SC states (weakly-gaped), which are protected by the time-reversal symmetry, are found at all other temperatures. The hugely gaped (bulk) excitonic state at $T = 50$ K and the T-dependence of the SC gap found in [1] showed that the hydrogenated graphitic system can host both bulk (characteristic to Bernal stacking) and flat-band surface states (characteristic to rhombohedral stacking).

In order to separate the SC component from the total DM component, the $m(B)$ data was replotted in two ways: 1) The difference between the magnetic moment at $T = 2.5$ K and the one at $T = 300$ K for both the H-C foil and the C foil (Fig. 7). While both the H-C foil and the C foil are more DM at $T =$ 2.5 K than at high $T = 300$ K, only the H-C foil shows a SC-like $m(B)$ loop and also the kink feature. The loop also starts from the origin, suggesting that the offset seen with the $m(B)$ loops is T-independent, thus FM. On the contrary, the offset in $m(B)$ is not canceled for the C foil, which is PM in a field. 2) The magnetic moment of the C foil was subtracted from the magnetic moment of the H-C foil (Fig. 8). Notice that at $T = 2.5$ K, the H-C foil is more DM than the C foil, while at $T = 300$ K the H-C foil is more FM than the C foil. Thus, the H-C foil is a FMSC, as already shown by Fig. 5.

IV. Conclusion

The results presented here on hydrogenated graphite foil are in agreement with our previous research, thus confirming HTSC

in hydrogenated graphitic materials with a $T_c \sim 50$–60 K for the main phase. By strengthening the magnetic field, the T-dependent magnetization reveals several important transitions: from a Néel PM-AFM transition, to a FMSC state, to an orbital PM glass HTSC. The magnetization loops show the kink feature characteristic to granular SC, in addition, FM extending up to room temperature. Long-range magnetic spin correlations favor the coexistence of magnetism and SC on the mesoscopic scale. Moreover, the topologically protected flat energy bands in H-C materials [1], [40] promote surface SC with T_c significantly higher than in the bulk. The magneto-structural phase transitions that we have just found [41] might indicate that the phase slips are cancelled by the high conductivity in the bulk graphite, thus leading to HTSC in the H-C materials. From the discovery of SC by Onnes in Hg with a $T_c \simeq 4.19$ K [42], the continuous quest for finding new HTSC materials and their likely spectrum scale many uses goes on.

ACKNOWLEDGEMENT

Nadina Gheorghiu acknowledges G.Y. Panasyuk for his continuous support and inspiration that made possible this publication.

REFERENCES

[1] N. Gheorghiu, C. R. Ebbing, and T. J. Haugan, "Superconductivity in Hydrogenated Graphites," 2020, doi: 10.48550/arXv.2005.05876.
[2] A. C. Basaran, J. E. Villegas, J. S. Jiang, A. Hoffmann, and I. K. Schuller, "Mesoscopic magnetism and superconductivity," *MRS Bull.*, vol. 40, pp. 925–932, Nov. 2015.
[3] M. S. Dresselhaus and G. Dresselhaus, "Intercalation compounds of graphite," *Adv. Phys.*, vol. 51, no. 1, pp. 1–186, 2002.
[4] Y. Kopelevich and P. Esquinazi, "Ferromagnetism and superconductivity in carbon-based systems," *J. Low Temp. Phys.*, vol. 146, no. 5/6, pp. 629–639, Mar. 2007.
[5] P. Esquinazi, A. Setzer, R. Hohne, and C. Semmelhack, "Ferromagnetism in oriented graphite samples," *Phys. Rev. B*, vol. 66, Jul. 2002, Art. no. 024429.
[6] S. Moehlecke, Y. Kopelevich, and M. B. Maple, "Local superconductivity and ferromagnetism interplay in graphite−sulfur composites," *Braz. J. Phys.*, vol. 33, no. 4, pp. 762–765, Dec. 2003.
[7] Y. Kopelevich, R. R. da Silva, J. H. S. Torres, S. Moehlecke, and M. B. Maple, "High-temperature local superconductivity in graphite and graphite-sulfur composites," *Physica C*, vol. 408-410, pp. 77–78, 2004.
[8] I. Felner, "Peculiar magnetic features and superconductivity in sulfur doped amorphous carbon," *Magnetochemistry*, vol. 2, Sep. 2016, Art. no. 34.
[9] A. Novac, V. V. Nguyen, E. Fischer, V. G. Lascu, and C. Q. Le, "A stable resistive transition in Y-Ba-Cu-O above 200 K," *Mater. Sci. Eng.: B*, vol. 34, no. 2-3, pp. 147–151, 1995.
[10] J. Bardeen, L. N. Cooper, and J. R. Schrieffer, "Theory of superconductivity," *Phys. Rev.*, vol. 108, no. 5, pp. 1175–1204, Dec. 1957.
[11] W. A. Little, "Possibility of synthesizing an organic superconductor," *Phys. Rev. A*, vol. 134, no. 6A, pp. A1416–A1424, Jun. 1964.
[12] Y. Kawashima and M. Iwamoto, "Protolytic decomposition of n-octane on graphite at near room temperature," *Sci. Rep.*, vol. 6, Jun. 2016, Art. no. 28493.
[13] Y. Kawashima, "Superconductivity above 500 K in conductors made by bringing n-alkane into contact with graphite," 2016, *arXiv:1612.05294*.
[14] N. Gheorghiu N, C. R. Ebbing, B. T. Pierce, and T. J. Haugan, "Quantum effects in graphitic materials: Colossal magnetoresistance, Andreev reflections, ferromagnetism, and granular superconductivity," *IOP Conf. Ser., Mater. Sci. Eng.*, vol. 756, Jul. 2020, Art. no. 012022.
[15] N. Gheorghiu, C. R. Ebbing, J. P. Murphy, B. T. Pierce, and T. J. Haugan, "Superconducting-like and magnetic transitions in oxygen-implanted diamond-like and amorphous carbon films, and in highly oriented pyrolytic graphite," *IOP Conf. Ser., Mater. Sci. Eng.*, vol. 1241, Jul. 2021, Art. no. 012054.
[16] N. Gheorghiu, C. R. Ebbing, and T. J. Haugan, "Boron content and the superconducting critical temperature of carbon-based materials," Dec. 2020, *arXiv:2012.06624*.
[17] N. Gheorghiu, C. R. Ebbing, and T. J. Haugan, "Electric-field induced strange metal states and possible high-temperature superconductivity in hydrogenated graphitic fibers," May 2020, *arXiv:2005.07885*.
[18] V. A. Kulbachinskii, "Coexistence of 2D weak localization and superconductivity in carbon fibers," *Synthetic Met.*, vol. 41-43, pp. 2697–2700, 1991.
[19] Y. G. Semenov, J. M. Zavada, and K. W. Kim, "Weak ferromagnetism of antiferromagnetic domains in graphene with defects," *Phys. Rev. B*, vol. 84, Oct. 2011, Art. no. 165435.
[20] O. V. Yazyev, "Emergence of magnetism in graphene materials and nanostructures," *Rep. Prog. Phys.*, vol. 73, Apr. 2010, Art. no. 056501.
[21] Y. Kubozono et al., "Superconductivity in aromatic hydrocarbons," *Physica C*, vol. 514, pp. 199–205, Feb. 2015.
[22] N. Gheorghiu, C. R. Ebbing, and T. J. Haugan, "Magnetism and superconductivity in hydrogenated graphite foils," Jun. 2022, *arXiv:2206.08562*.
[23] Y. Yeshurun, I. Felner, and H. Sompolinsky, "Magnetic properties of a high-T_c superconductor $YBa_2Cu_3O_7$: Reentrylike features, paramagnetism, and glassy behavior," *Phys. Rev. B*, vol. 36, no. 1, pp. 840–842, Jul. 1987.
[24] E. R. Podolyak, "On magnetic flux trapping by surface superconductivity," *J. Exp. Theor. Phys.*, vol. 126, no. 3, pp. 389–396, 2018.
[25] A. K. Geim, S. V. Dubonos, J. G. S. Lok, M. Henini, and J. C. Maan, "Paramagnetic meissner effect in small superconductors," *Nature*, vol. 396, pp. 144–146, Nov. 1998.
[26] L. A. B. Olde Olthof, X. Montiel, J. W. A. Robinson, and A. I. Buzdin, "Superconducting vortices generated via spin-orbit coupling at superconductor/ferromagnet interfaces," *Phys. Rev. B*, vol. 100, Dec. 2019, Art. no. 220505(R).
[27] W. Braunisch et al., "Paramagnetic Meissner effect in high-temperature superconductors," *Phys. Rev. B*, vol. 48, no. 6, Apr. 1993, Art. no. 4030.
[28] D. Domínguez, E. A. Jagla, and C. A. Balseiro, "Wohlleben effect in a model granular high TC superconductor," *Physica C*, vol. 235-240, pp. 3283–3284, 1994.
[29] W. A. Ortiz, P. N. Lisboa-Filho, W. A. C. Passos, and F. M. Araujo-Moreira, "Field-induced networks of weak-links: An experimental demonstration that the paramagnetic Meissner effect is inherent to granularity," *Physica C*, vol. 361, pp. 267–273, Apr. 2001.
[30] S.-I. Suzuki and Y. Asano, "Paramagnetic instability of small topological superconductors," *Phys. Rev. B*, vol. 89, May 2014, Art. no. 184508.
[31] S.-I. Suzuki, T. Hirai, M. Eschrig, and Y. Tanaka, "Anomalous inverse proximity effect in unconventional superconductor junctions," *Phys. Rev. Res.*, vol. 3, Dec. 2021, Art. no. 043148.
[32] E. Lake and T. Senthil, "Reentrant superconductivity through a quantum Lifshitz transition in twisted trilayer graphene," *Phys. Rev. B*, vol. 104, Nov. 2021, Art. no. 174505.
[33] G. E. Volovik, "Graphite, graphene and the flat band superconductivity," *JETP Lett.*, vol. 10, no. 8, pp. 516–517, Apr. 2018.
[34] S. Layek et al., "Possible high temperature superconducting transitions in disordered graphite obtained from room temperature deintercalated KC_8," *Carbon*, vol. 201, pp. 667–668, Sep. 2022.
[35] F. V. Kusmartsev, "Orbital glass in HTSC: A new state of condensed matter," *J. Supercond. Novel Magnetism*, vol. 5, no. 5, pp. 463–469, May 1992.
[36] N. Garcia and P. Esquinazi, "Mean-field superconductivity approach in two dimensions," *J. Supercond. Novel Magnetism*, vol. 22, pp. 439–444, Apr. 2009.
[37] S. Kumar, R. P. Singh, A. Thamizhavel, and C. V. Tomy, "Evidence of surface superconductivity and multi-quanta vortex state in a weakly-pinned single crystal of $Ca_3Ir_4Sn_{13}$," *Physica C*, vol. 509, pp. 42–48, Dec. 2014.
[38] W. A. C. Passos et al., "Granularity in superconductors: Intrinsic properties and processing-dependent effects," *Physica C*, vol. 354, pp. 189–196, 2001.
[39] D. Saint-James and P. G. deGennes, "Onset of superconductivity in decreasing fields," *Phys. Lett.*, vol. 7, no. 5, pp. 306–308, Nov. 1963.
[40] N. Gheorghiu, C. R. Ebbing, and T. J. Haugan, "Flat-band energy analysis of the superconducting gap for hydrogenated graphite fibers found from nonlocal electrical conductance experimental data," Feb. 2023, *arXiv:2302.0064*.
[41] N. Gheorghiu, C. R. Ebbing, and T. J. Haugan, "Magneto-structural phase transitions and two-dimensional spin waves in graphite," *IOP Conf. Ser., Mater. Sci. Eng.*, vol. 1302, Jul. 2024, Art. no. 012034.
[42] H. Kamerlingh Onnes, *Commun. Phys. Lab. Univ. Leiden*, vol. 12, no. 120, 1911.